Correlation between nuclear temperature and symmetry energy in subsaturation nuclear matter density

Fan Zhang [●],[1,*] Kai-Lei Wang,[1] Li-Ding Jin,[1] Zhu-Li Zhang,[1] Hui-Xiao Duan,[1] and Cheng Li[2,3,†]

[1]*Department of Physics, Changzhi University, Changzhi 046011, People's Republic of China*
[2]*Department of Physics, Guangxi Normal University, Guilin 541004, People's Republic of China*
[3]*Guangxi Key Laboratory of Nuclear Physics and Technology, Guilin 541004, People's Republic of China*

Herein, a study of the correlation between nuclear temperature and symmetry energy is presented for heavy ion collisions at intermediate energies via the isospin-dependent quantum molecular-dynamics model. It is found that different symmetry energy parameters change the density and kinetic energy distribution of the hot nuclei. More importantly, nuclear temperatures that are based on kinetic energy properties can be used to study symmetry energy information.

I. INTRODUCTION

Nuclear symmetry energy, which has been a research focus of nuclear physics for many years, governs important properties of nuclei and neutron stars [1]. Compared to regions with saturation density, the large uncertainties in symmetry energy exist in low- and high-density regions. To reduce the uncertainties regarding symmetry energy in non-saturated density regions, many investigations have been undertaken; at subsaturation densities, these include isotopic scaling [2,3], isospin fractionation [4,5], pre-equilibrium single and double neutron-proton ratios [6–9], isobaric ratios of various species [10], and giant dipole resonance (GDR) [11–14]. However, the high-density behavior of symmetry energy has been studied using methods such as collective and elliptic flows [15–17], neutron-proton ratios of free nucleons [18,19], π^-/π^+ [20,21], and K^+/K^0 [22]. The divergence of symmetry energy is larger in high-density regions than in low-density regions. To constrain symmetry energy, π^-/π^+ has attracted increasing attention. The ratio π^-/π^+ was first discussed in terms of Coulomb effects by Bertsch *et al.* [23]. Accordingly, Bonasera *et al.* further found that π^-/π^+ carried the information of symmetry energy [24]. However, the ratio π^-/π^+ is affected by the momentum-dependent interaction, threshold effect, and pion potential [25], among other factors. Thus, theoretical calculations resulted in different symmetry energies. Numerous efforts have been directed toward constraining symmetry energy, but further studies are needed to improve the accuracy of the constraint on symmetry energy at sub- and suprasaturation densities.

Recent experimental and theoretical studies show that nuclear temperatures have isospin dependence [26–31]. Two main factors contribute to this phenomenon: the Coulomb interaction and symmetry energy. Based on Landau theory, McIntosh *et al.* revealed a linear dependence of temperature on Coulomb energy and symmetry energy [27]. Therefore, if one could select appropriate hot nuclei and reduce the effects of the Coulomb interaction, one might use the nuclear temperature isospin dependence to study symmetry energy. In this work, we focus on symmetry energy at subsaturation densities and examine the correlation between nuclear temperature and symmetry energy in low-density regions.

II. MODEL AND METHODS

We attempted to study the correlation between nuclear temperature and symmetry energy in a low-density region via the isospin-dependent quantum molecular-dynamics (IQMD) model [32–35] incorporating the statistical GEMINI decay model [36]. To better connect the two models, we required a dynamical model to describe the intermediate-mass-fragment (IMF) emission. When the maximum fragment excitation energy is less than a certain value E_{stop}, the dynamic simulation stops and the statistical decay model will completes the decay of pre-fragments. The value of E_{stop} corresponds to the threshold energy for IMF emission. In this work, $E_{stop} = 2$ MeV/nucleon. Using this value, the experimental data for IMF production can be described very well [34].

In the present model, the Hamiltonian H is expressed as

$$H = \tau + U_{\text{Coul}} + \int V(\rho)dr, \tag{1}$$

where τ is the kinetic energy and U_{Coul} the Coulomb potential energy. $V(\rho)$ is the nuclear potential energy density function, which is written as

$$V(\rho) = \frac{\alpha}{2}\frac{\rho^2}{\rho_0} + \frac{\beta}{\gamma+1}\frac{\rho^{\gamma+1}}{\rho_0^{\gamma}} + \frac{\text{g}_{\text{sur}}^{\text{iso}}}{2}\frac{(\nabla\rho_n - \nabla\rho_p)^2}{\rho_0}$$
$$+ \frac{\text{g}_{\text{sur}}}{2}\frac{(\nabla\rho)^2}{\rho_0} + \text{g}_{\tau}\frac{\rho^{8/3}}{\rho_0^{5/3}} + \frac{C_{\text{sym}}}{2}\left(\frac{\rho}{\rho_0}\right)^{\gamma_i}\rho\delta^2. \tag{2}$$

*zhangfan@czc.edu.cn
†licheng@mail.bnu.edu.cn

The parameters used in this study are $\alpha = -168.40$ MeV, $\beta = 115.90$ MeV, $\gamma = 1.50$, $g_{\text{sur}} = 92.13$ MeV fm^2, $g_{\text{sur}}^{\text{iso}} = -6.97$ MeV fm^2, $C_{\text{sym}} = 38.13$ MeV, and $g_\tau = 0.40$ MeV. The corresponding compressibility is 271 MeV [37]. In this work, we used three symmetry parameters, $\gamma_i =0.5$, 1.0, and 2.0, which correspond to soft, linear, and hard symmetry energy, respectively.

To study the energy distribution of the hot nuclei, we must find them in the early stage of the reactions from the phase space. Hot nuclei can be selected by the relative distance (R_p) among the nucleons. If the relative distance between two nucleons is smaller than R_p, then they can be recognized as belonging to one cluster. In this work, $R_p = 3$ fm, which is the typical value of nuclear force scope. To further select the equilibrated projectile spectator, spherical spectators are selected by the ratio of parallel to transverse quantities:

$$Q_{\text{shape}} = \frac{2 \sum_i p_{zi}^2}{\sum_i \left(p_{xi}^2 + p_{yi}^2 \right)}, \quad (3)$$

where p_{xi}, p_{yi}, and p_{zi} are the momentum components of the ith nucleon along the x, y, and z axes, respectively, in the center-of-mass frame of the projectile spectator. If the Q_{shape} value of the spectator satisfies $-0.3 \leqslant \log_{10}(Q_{\text{shape}}) \leqslant 0.3$, then the spectator is a candidate that may be used to study thermodynamic properties. To use the spectator to study nuclear temperature, the mass and neutron-proton ratio requirement must also be met, because a large mass and neutron-proton ratio range will affect the nuclear temperature isospin effects measurement [38]. To reduce the effects of mass and the neutron-proton ratio on the nuclear temperature measurement, the mass and neutron-protons ratio range of hot nuclei should be $185 \leqslant A \leqslant 195$ and $1.3 \leqslant N/Z \leqslant 1.4$, respectively.

When the hot nuclei are identified, their excitation energy and temperature can be calculated. The excitation energy E^* of the hot nuclei is calculated by

$$E^* = \tau + V - B, \quad (4)$$

where τ and V are the kinetic and potential energy of the hot nuclei, respectively, and B is the binding energy of the hot nuclei at the ground state. The temperatures of the spectator are calculated by the momentum quadrupole temperature [39]:

$$\langle \sigma_{xy}^2 \rangle = 4m^2 T^2, \quad (5)$$

where m is the probe particle mass, and $\langle \sigma_{xy}^2 \rangle$ is the variance of the momentum quadrupole.

III. RESULTS AND DISCUSSION

The early test for the symmetry energy by collective motion is the GDR [12]. Using the GDR, different symmetry energies have been obtained [13,14,40]. Those calculations clearly show that the GDR is sensitive to the symmetry energy, but different symmetry energies and densities. Trippa *et al.* found that the GDR is strongly correlated with the symmetry energy around density 0.1 fm^{-3} [14]. In another reference, the GDR is found to be sensitive to the symmetry energy at density 0.02 fm^{-3} [13]. There is a debate about which density region symmetry energy dominates the GDR. As a result,
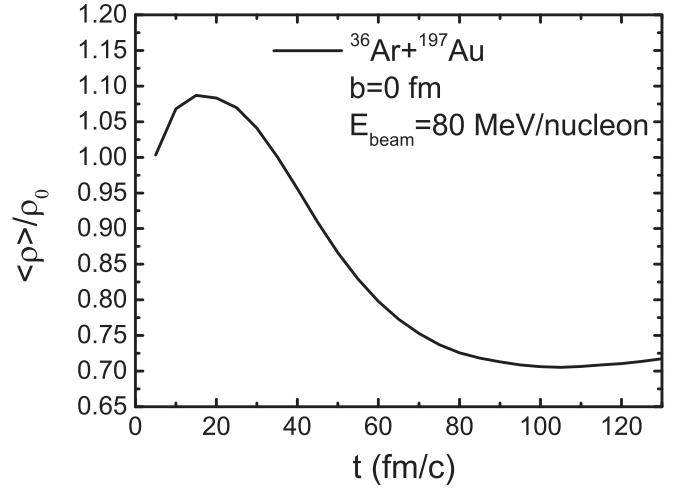

FIG. 1. Time evolution of the largest cluster average density.

the strengths of symmetry energy are different for different calculations. Using the GDR to study symmetry energy is also affected by different Skyrme parametrizations and effective mass splitting [14,40]. Therefore, studies of other observables are needed. In the present work, we use the difference in collective expansion which is caused by symmetry energy, to study symmetry energy.

Figure 1 shows the time evolution of the largest-cluster average density, in which the reaction system is ^{36}Ar + ^{197}Au at 80 MeV/nucleon with central collisions. It is worth mentioning that the largest cluster is not the same as the hot nuclei that are used to calculate energy distribution and nuclear temperature. When the Q_{shape}, mass, and N/Z values meet the requirements of hot nuclei, the largest cluster is a hot nucleus, and will be used in the next step of this study. It can be seen from Fig. 1 that the largest-cluster average density reaches the maximum value of approximate 20 fm/c. At this moment, the reaction system reaches maximum compression. After 20 fm/c, the largest-cluster average density decreases with reaction time, which is caused by the expansion of the reaction system. When the momentum distribution of the largest cluster reaches isotropy (approximate 110 fm/c [29]), the largest cluster is a candidate for a hot nucleus, which can be used to study nuclear temperature. The average density of the hot-nuclei candidates is in the subsaturation density region and is approximately $0.7\rho_0$. If one studies the temperature of hot nuclei, then the nuclear temperatures should carry the information about nuclear symmetry energy at subsaturation densities. It can be seen from Fig. 1 that the average density of the largest cluster is below saturation density ($0.7\rho_0 < \rho < 0.9\rho_0$) in the formation process (50 fm/c < t). In this density region, the pressure caused by symmetry energy is positive. As such, the role of symmetry energy is to make it easier for the system to expand.

The pressure of the symmetry energy can be written as

$$P_{\text{sym}} = \rho^2 \left(\frac{\partial e_{\text{sym}}}{\partial \rho} \right)_{T, \delta = \text{constant}}, \quad (6)$$
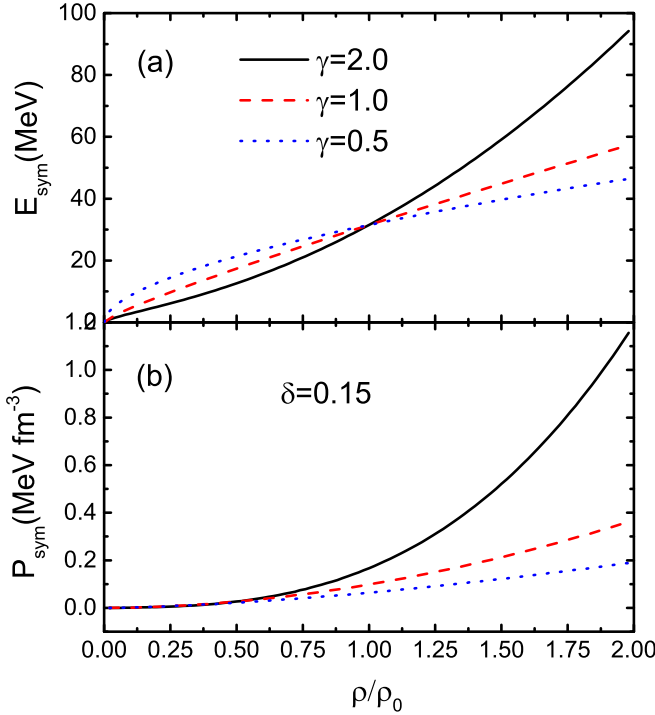
FIG. 2. Symmetry energy (a) and pressure of symmetry energy (b) as function of density for isospin asymmetry of $\delta = 0.15$ and γ_i parameters of 0.5, 1.0, and 2.0, respectively.

where e_{sym} is $E_{sym}\delta^2$. In the present work, $\delta = 0.15$, which corresponds to hot nuclei neutron-proton asymmetry. Since the pressure increases with the slope of symmetry energy, it can be seen from Fig. 2(b) that the hard ($\gamma_i = 2.0$) symmetry energy leads to a larger pressure than the soft symmetry energy ($\gamma_i = 0.5$) at densities above $0.7\rho_0$. The hot nuclei with hard symmetry energy will be much easier to expand. Therefore, the density of the hot nuclei that use hard symmetry energy should be the lowest. To show the effects of symmetry energy on the hot-nuclei properties, the density and energy distribution are compared in Figs. 3 and 4 at 110 fm/c.

The density versus excitation energy of hot nuclei is shown in Fig. 3. To obtain hot nuclei with different excitation energies, the reaction systems ^{36}Ar + ^{197}Au at 70, 75, and 80 MeV/nucleon with different symmetry energy parameters are used. It can be seen from Fig. 3 that the average density is the lowest for the hard symmetry energy, which supports the above reasoning. It can also be seen from Fig. 3 that the density decreases with increasing excitation energy. Using the same symmetry energy, the hot nuclei will expand more easily with higher excitation energy. A similar result was obtained by Wuenschel *et al*. [39].

To further investigate the correlation between symmetry energy and nuclear temperature, the energy distribution of hot nuclei is shown in Fig. 4, in which the average total energy E_{tot} of the hot nuclei is divided into three parts, namely, average potential energy E_{pot}, collective kinetic energy E_{coll}, and intrinsic kinetic energy E_{int},

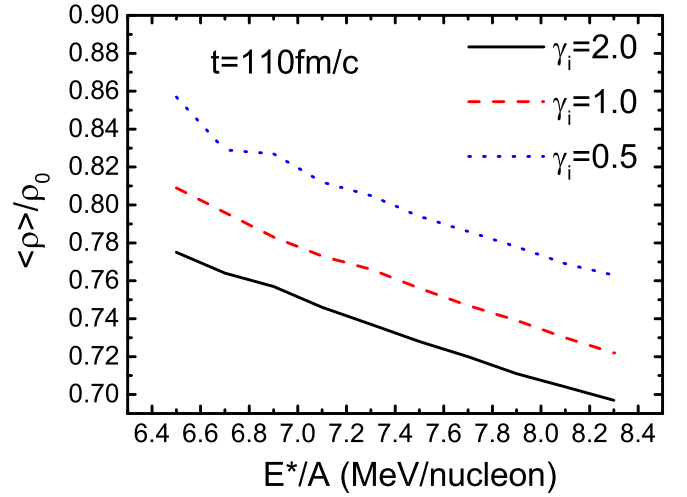$$E_{tot} = E_{pot} + E_{coll} + E_{int}. \tag{7}$$

FIG. 3. Hot-nuclei average density as a function of excitation energy for different asymmetry parameters.
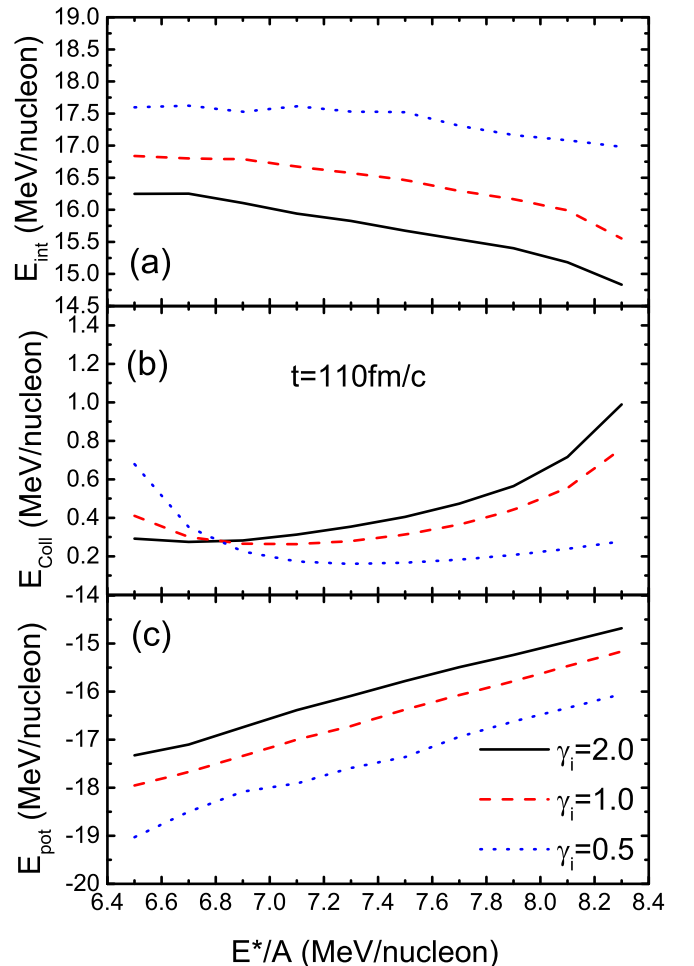

FIG. 4. Intrinsic kinetic energy (a), collective kinetic energy (b), and potential energy (c) as a function of excitation energy.
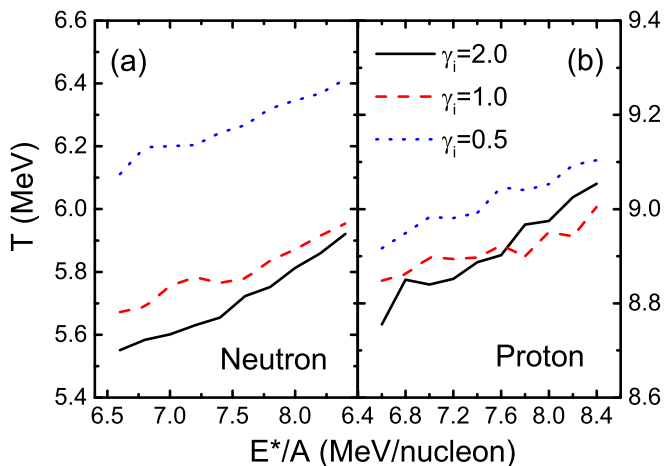
FIG. 5. Nuclear temperature of hot nuclei as function of excitation energy for different asymmetry parameters.

E_{int} includes Fermi kinetic energy and thermal kinetic energy. The difference between Fermi motion and thermal motion comes from the change of hot-nuclei density, which carries symmetry energy information.

It can be seen from Fig. 4 that the potential energy per nucleon is the highest for hard symmetry energy. This is due to the hot nuclei with hard symmetry energy having the lowest densities (see Fig. 3). The difference in the potential energy among the different symmetry energies is approximately 2 MeV/nucleon. Compared to the potential energy, the difference in the collective kinetic energy is weak. Furthermore, the difference in E_{coll} is approximately 0.2–0.6 MeV/nucleon for different excitation energies. For hot nuclei that have the same excitation energy, the intrinsic kinetic energy will be higher for hot nuclei with soft symmetry energy. It can be seen from Fig. 4(a) that the difference in E_{int} among different symmetry energies is approximately 2 MeV/nucleon; the E_{int} value is higher for soft symmetry energy. It is worth mentioning

that E_{int} at 110 fm/c is not particle kinetic energy which is measured by experiment, because the emitted particles must overcome potential energy attraction. However, the emitted particles still carry the information of E_{int} and reflect the difference of symmetry energy. Therefore, the difference in E_{int} among the different symmetry energies is expressed by particle momentum. Based on the classical Maxwell distribution, the nuclear temperature can be calculated by Eq. (5). In Fig. 5, neutrons and protons were selected as the probe particles, the yields of which are enough to satisfy statistical requirements. It can be found from Fig. 5(a) that the softer the symmetry parameter, the higher the hot-nuclei temperature. Compared to neutrons, the difference in nuclear temperature among different symmetry energies is weak when protons are used [Fig. 5(b)]. This is mainly caused by the Coulomb effect. After the neutrons and protons are created, the momentum of protons is changed by Coulomb force. Since thermonuclear information carried by protons is affected, the influence of the Coulomb effect should be minimized when classical momentum quadrupole temperatures are used to extract symmetry energy information at the subsaturation density region.

IV. CONCLUSIONS

In this study, we presented the details of a study of the relation between the momentum quadrupole temperature and symmetry energy using the IQMD model. We found that using different symmetry energies, the energy distribution and average density of hot nuclei were changed. Interestingly, a strong correlation existed between the "classical" momentum quadrupole temperature and symmetry energy in the subsaturation density region.

[1] B.-A. Li, L.-W. Chen, and C. M. Ko, Phys. Rep. **464**, 113 (2008).

[2] D. V. Shetty, S. J. Yennello, and G. A. Souliotis, Phys. Rev. C **75**, 034602 (2007).

[3] M. B. Tsang, W. A. Friedman, C. K. Gelbke, W. G. Lynch, G. Verde, and H. Xu, Phys. Rev. Lett. **86**, 5023 (2001).

[4] M. B. Tsang, T. X. Liu, L. Shi, P. Danlelewicz, C. K. Gelbke, X. D. Liu, W. G. Lynch, W. P. Tan, G. Verde, A. Wagner, H. S. Xu, W. A. Friedman, L. Beauliwu, B. Davin, R. T. de Souza, Y. Larochelle, T. Lefort, R. Yanez, V. E. Viola, R. J. Charity, and L. G. Sobotka, Phys. Rev. Lett. **92**, 062701 (2004).

[5] A. Ono, P. Danielewicz, W. A. Friedman, W. G. Lynch, and M. B. Tsang, Phys. Rev. C **68**, 051601(R) (2003).

[6] Y. Zhang, P. Danielewicz, M. Famiano, Z. Li, W. G. Lynch, and M. B. Tsang, Phys. Lett. B **664**, 145 (2008).

[7] B. A. Li, C. M. Ko, and Z. Ren, Phys. Rev. Lett. **78**, 1644 (1997).

[8] S. Kumar, Y. G. Ma, G. Q. Zhang, and C. L. Zhou, Phys. Rev. C **84**, 044620 (2011).

[9] M. B. Tsang, Z. Chajecki, D. Coupland, P. Danielewicz, F. Famiano, R. Hodges, M. Kilburn, F. Lu, W. G. Lynch, J. Winkelbauer, M. Youngs, and Y. X. Zhang, Prog. Part. Nucl. Phys. **66**, 400 (2011).

[10] C. W. Ma, F. Wang, Y. G. Ma, and C. Jin, Phys. Rev. C **83**, 064620 (2011).

[11] S. Mordechai, H. T. Fortune, J. M. O'Donnell, G. Liu, M. Burlein, A. H. Wuosmaa, S. Greene, C. L. Morris, N. Auerbach, S. H. Yoo, and C. F. Moore, Phys. Rev. C **41**, 202 (1990).

[12] R. ö. Akyüz and S. Fallieros, Phys. Rev. Lett. **27**, 1016 (1971).

[13] J. Su, Chin. Phys. C **43**, 064109 (2019).

[14] L. Trippa, G. Colò, and E. Vigezzi, Phys. Rev. C **77**, 061304(R) (2008).

[15] S. Gautam, R. Kumari, and R. K. Puri, Phys. Rev. C **86**, 034607 (2012).

[16] S. Gautam, A. D. Sood, R. K. Puri, and J. Aichelin, Phys. Rev. C **83**, 034606 (2011).

[17] P. Russotto, P. Z. Wu, M. Zoric, M. Chartier, Y. Leifels, R. C. Lemmon, Q. Li, J. Lukasik, A. Pagano, P. Pawlowski, and W. Trautmann, Phys. Lett. B **697**, 471 (2011).

[18] G. C. Yong, B. A. Li, and L. W. Chen, Phys. Lett. B **650**, 344 (2007).

[19] S. Kumar, Y. G. Ma, G. Q. Zhang, and C. L. Zhou, Phys. Rev. C **85**, 024620 (2012).

[20] B. A. Li, W. J. Guo, and Z. Shi, Phys. Rev. C **91**, 044601 (2015).

[21] Z. Xiao, B. A. Li, L. W. Chen, G. C. Yong, and M. Zhang, Phys. Rev. Lett. **102**, 062502 (2009).

[22] Q. Li, Z. Li, S. Soff, R. K. Gupta, M. Bleicher, and H. Stocker, J. Phys. G: Nucl. Part. Phys. **31**, 1359 (2005).

[23] G. Bertsch, Nature (London) **283**, 280 (1980).

[24] A. Bonasera and G. F. Bertsch, Phys. Lett. B **195**, 521 (1987).

[25] Y. Liu, Y. Wang, Y. Cui, C. J. Xia, Z. Li, Y. Chen, Q. Li, and Y. Zhang, Phys. Rev. C **103**, 014616 (2021).

[26] C. Sfienti, P. Adrich, T. Aumann, C. O. Bacri, T. Barczyk, R. Bassini, S. Bianchin, C. Boiano, A. S. Botvina, A. Boudard, J. Brzychczyk, A. Chbihi, J. Cibor, B. Czech, M. De Napoli, J. E. Ducret, H. Emling, J. D. Frankland, M. Hellstrom, D. Henzlova, G. Imme, I. Iori, H. Johansson, K. Kezzar, A. Lafriakh, A. Le Fevre, E. Le Gentil, Y. Leifels, J. Luhning, J. Lukasik, W. G. Lynch, W. Lynen, Z. Majka, M. Mocko, W. F. J. Muller, A. Mykulyak, H. Orth, A. N. Otte, P. Palit, P. Pawlowski, A. Pullia, G. Raciti, E. Rapisarda, H. Sann, C. Schwarz, H. Simon, K. Summerer, W. Trautmann, M. B. Tsang, G. Verde, C. Volant, M. Wallace, H. Weick, J. Wiechula, A. Wieloch, and B. Zwieglinski, Phys. Rev. Lett. **102**, 152701 (2009).

[27] A. B. McIntosh, A. Bonasera, P. Cammarata, K. Hagel, L. Heilborn, Z. Kohley, J. Mabiala, L. W. May, P. Marini, A. Raphelt, G. Z. Souliotis, S. Wuenschel, A. Zarrella, and S. J. Yennello, Phys. Lett. B **719**, 337 (2013).

[28] J. Su and F.-S. Zhang, Phys. Rev. C **84**, 037601 (2011).

[29] F. Zhang, C. Li, P.-W. Wen, J.-W. Liu, J. Su, and F.-S. Zhang, Phys. Rev. C **100**, 024603 (2019).

[30] F. Zhang, C. Li, L. Zhu, H. Liu, and F.-S. Zhang, Phys. Rev. C **91**, 034617 (2015).

[31] R. Ogul and A. S. Botvina, Phys. Rev. C **66**, 051601(R) (2002).

[32] J. Aichelin, Phys. Rep. **202**, 233 (1991).

[33] C. Hartnack, Z. X. Li, L. Neise, G. Peilert, A. Rosenhauer, H. Sorge, J. Aichelin, H. Stöcker, and W. Greiner, Nucl. Phys. A **495**, 303 (1989).

[34] F. Zhang and J. Su, Chin. Phys. C **43**, 024103 (2019).

[35] F. Zhang and J. Su, Nucl. Sci. Tech. **31**, 77 (2020).

[36] R. J. Charity, M. A. McMahan, G. J. Wozniak, R. J. McDonald, L. G. Moretto, D. G. Sarantites, L. G. Sobotka, G. Guarino, A. Pantaleo, L. Fiore, A. Gobbi, and K. D. Hildenbrand, Nucl. Phys. A **483**, 371 (1988).

[37] B. A. Brown, Phys. Rev. C **58**, 220 (1998).

[38] H. X. Duan, D. H. Zhang, F. Zhang, and H. S. Wu, Nucl. Phys. A **1009**, 122156 (2021).

[39] S. Wuenschel, A. Bonasera, L. W. May, G. A. Souliotis, R. Tripathi, S. Galanopoulos, Z. Kohley, K. Hagel, D. V. Shetty, K. Huseman, S. N. Soisson, B. C. Stein, and S. J. Yennello, Nucl. Phys. A **843**, 1 (2010).

[40] H. Y. Kong, J. Xu, L. W. Chen, B. A. Li, and Y. G. Ma, Phys. Rev. C **95**, 034324 (2017).